Endosomal Leakage and Nuclear Translocation of Multiwalled Carbon Nanotubes: Developing a Model for Cell Uptake

SUPPORTING INFORMATION

Qingxin Mu[1,2], Dana Broughton[2], Bing Yan[1,2 *]

Table of Contents

1. Materials and Methods

1.1. Materials. MWCNT-COOHs were made as reported (Zhou et al., Nano Lett. 8, 859). HEK293 (human embryonic kidney epithelial) cells were grown in Dulbecco's Minimum Essential Medium (DMEM, Gibco, Grand Island, NY) supplemented with 10% heat-inactivated fetal bovine

serum (Invitrogen, Carlsbad, CA), 2 mM L-glutamine, 100 μg/mL penicillin and 100 U/mL streptomycin. Guava ViaCount reagent (Millipore, Billerica, MA) was used for cell growth assay. Human Plasma was purchased from Innovative Research (Novi, MI). Other chemicals were purchased from Sigma Aldrich (St. Louis, MO).

1.2. Synthesis of MWCNT-NH_2. For a typical modification of MWCNT-COOH to MWCNT-NH_2, 1000 mg of MWCNT-COOH was dissolved in 25 mL of Thionyl Chloride (344 equivalents) and 10 mL of Dimethyl Formamide (DMF). The reaction was heated to 75°C and refluxed overnight. The reaction was allowed to cool and the thionyl chloride and DMF were removed through rotary evaporation. The nanotubes were dissolved in 300 mL of methylene chloride and 15 mL of 1, 3-diaminopropane was slowly added to the reaction mixture. The reaction was refluxed at 40°C overnight. The reaction was allowed to cool and the solvent was removed through rotary evaporation. The nanotubes were suspended in methanol and washed through an ultrasonic redispersion-centrifugation to remove impurities. The ultrasonic redispersion-centrifugation was repeated with several solvents including methanol, water, and ethanol 8 times. The excess solvent was then removed via vacuum. The nanotubes were characterized through FT-IR, elemental analysis and zeta potential. The FT-IR data showed a disappearance of peaks between 3000 and 2500, 2000, 1400 with the appearance of peaks around 3300, 1770, 1000, and 1500 with the conversion from MWCNT-COOH and MWCNT-NH_2 (SI_Figure 1). The zeta potential of the MWCNT-COOH shifted from -57 mV to 26 mV with the amine functionalization. The elemental analysis of the nanotubes shifted from <0.5% of nitrogen with the MWCNT-COOH to approximately 2.8% with the MWCNT-NH_2.

1.3. Transmission Electron Microscopy (TEM). HEK293 cells were treated with 100 μg/mL MWCNTs for one hour and 48 hours respectivley. Then cells were fixed in 2.5% glutaraldehyde in 0.1M sodium cacodylate buffer (pH 7.4) for one hour in room temperature and rinsed. Cells were then post fixed one hour in 2% osmium tetroxide with 3% potassium ferrocyanide and rinsed, next enbloc

staining with a 2% aqueous uranyl acetate solution and dehydration through a graded series of alcohol, two changes of propylene oxide, a series of propylene oxide/epon dilutions and embedded in 100% epon. The thin (70 nm) sections were cut on a Leica UC6 ultramicrotome and images were taken on a JEOL 1200 EX (JEOL, Ltd. Tokyo, Japan) using an AMT 2k digital Camera.

1.4. Identification of MWCNT bound proteins by LC-MS/MS. MWCNTs (400 μg/mL) were incubated with human plasma proteins (20%) in PBS overnight. Mixture was centrifuged and washed with PBS four times (16,000 g, 30 minutes for first time followed by 10 minutes three times). Pellet was collected and MWCNT bound proteins were digested in solution using trypsin enzyme (Promega, Madison, WI) (12hr, 37°C). The resulting peptide mixture was acidified to pH3.5 with formic acid and fractionated by nanoflow reversed-phase ultra high-pressure liquid chromatography on nanoAcquity ultra performance LC system (Waters Corporation, Milford, MA). Tryptic peptides were loaded onto a "precolumn" (Symmetry C18, 180μm i.d X 20mm, 5μm particle) (Waters Corporation, Milford, MA) which was connected through a zero dead volume union to the analytical column (BEH C18, 75μm i.d X 100mm, 1.7μm particle) (Waters Corporation, Milford, MA). Tryptic peptides were eluted over a 86 minutes gradient (0-70% B in 70 minutes, 70-100% B in 86minutes, where B = 70% Acetonitrile, 0.2% formic acid) at a flow rate of 250nL/min and introduced online into a linear ion trap mass spectrometer (Thermo Fisher, San Jose, CA) using electrospray ionization (ESI). Data dependent scanning was incorporated to select abundant precursor ions for fragmentation by acquisition of a full-scan mass spectrum followed by MS/MS on the 10 most abundant ions (one microscan per spectra; precursor m/z ± 1.5Da, 35% collision energy, 30ms ion activation, 35s dynamic exclusion, repeat count 2).

Product ions generated by fragmentation along the peptide backbone by collision activated dissociation (CAD) (b/y-type ions) were used in an automated database search against the Swissprot database using Mascot search routine with following residue modifications being allowed: Cysteine

(Carbamidomethylation), and Methionine (Oxidation). Database search results were verified by manual inspection of matches.

1.5. Cell uptake of MWCNTs monitored by flow cytometry and epifluorescence. MWCNT (2.0 mg) was dissolved into 2 mL deionized water by sonication for 20 minutes. FITC-BSA (2.0 mg) was dissolved in 2 mL PBS. MWCNT and FITC-BSA were mixed with gently pepitting. MWCNT/FITC-BSA mixture was incubated at 4°C overnight. Free FITC-BSA was removed through centrifuge (16,000g, 30 min) and washing. MWCNT/FITC-BSA was re-suspended in deionized water; HEK293 cells were incubated with ~100 μg/mL MWCNT/FITC-BSA for one hour. Cells were then loaded into flow cytometer for analysis. The suspending cells were also imaged using epifluorescence microscope. Green signal was collected or imaged in detections.

1.6. Cell Growth. Cell growth was monitored by flow cytometry. Nanotube suspensions were added to wells 24 hours after HEK293 cells seeded. The final concentrations of nanotubes were 12.5, 25, 50 and 100 μg/mL. After 48 hours, cells were harvested and labeled with Guava ViaCount reagent which differentially stained viable and non-viable cells based on their permeability to DNA-binding dyes in the reagent. Viable and dead cell populations were analyzed using Guava Easycyte Mini system with Guava Cytosoft software (Millipore, Billerica, MA). Each measurement was triplicated.

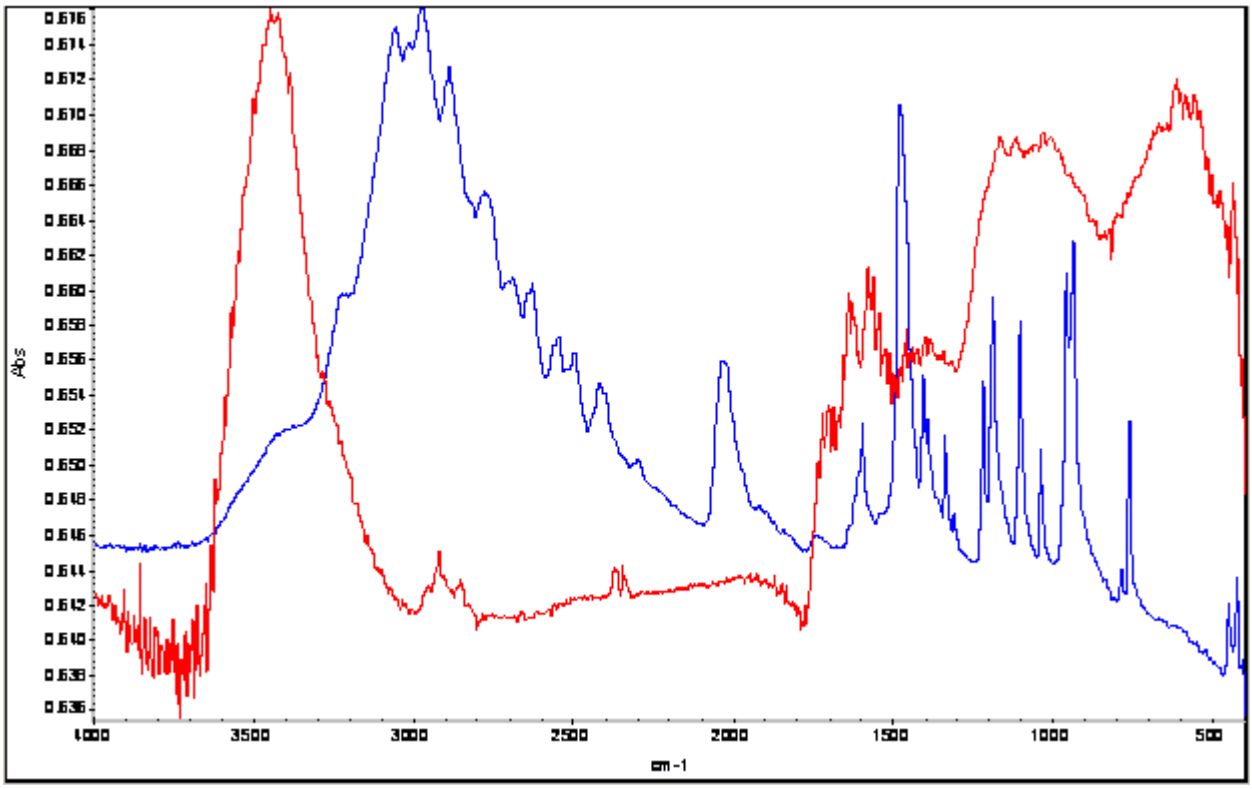

Figure S1. FT-IR analysis of MWCNT-COOH (blue) and MWCNT-NH_2 (red).

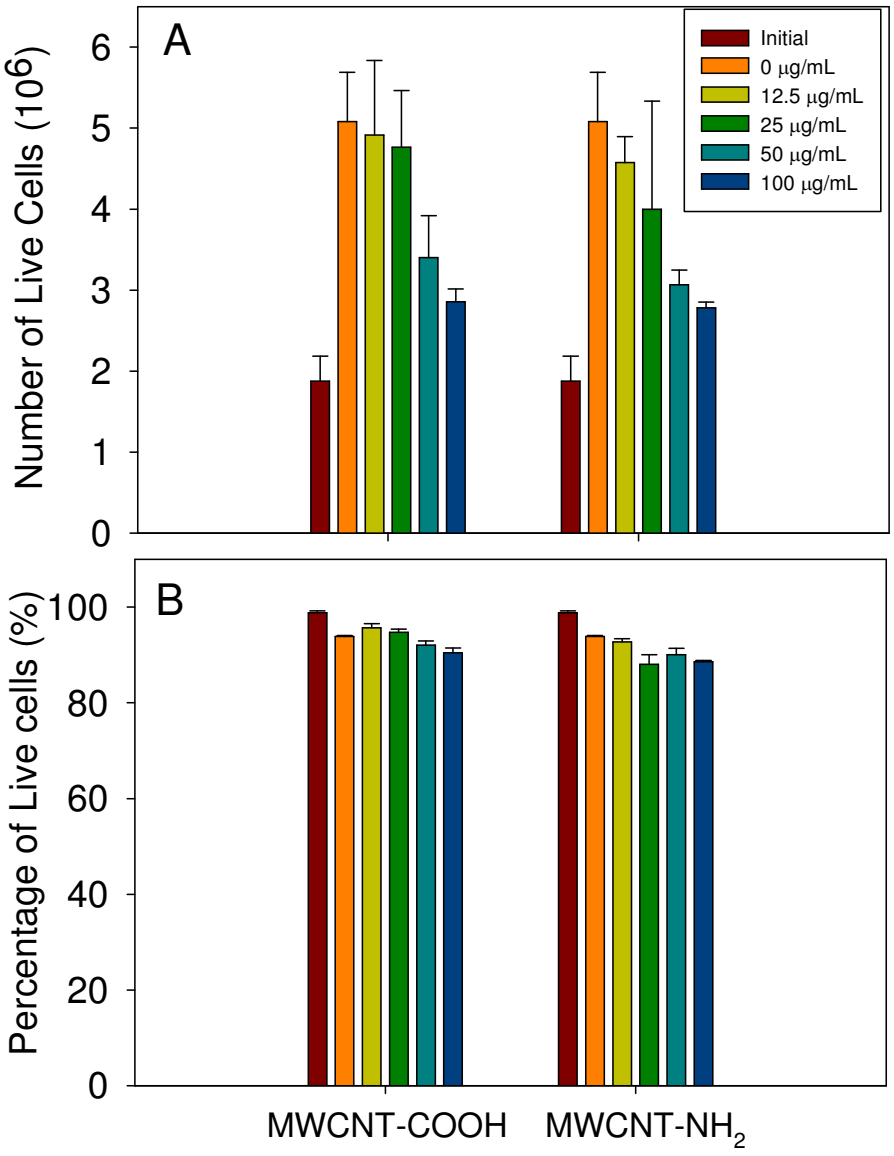

Figure S2. Influence of MWCNTs on cell growth. A. Live cell number counting 48 hours after MWCNTs addition; B. Percentage of live cells in total cell counting 48 hours after MWCNTs addition. "Initial" indicates the counting of cell numbers at the time point of MWCNTs addition.

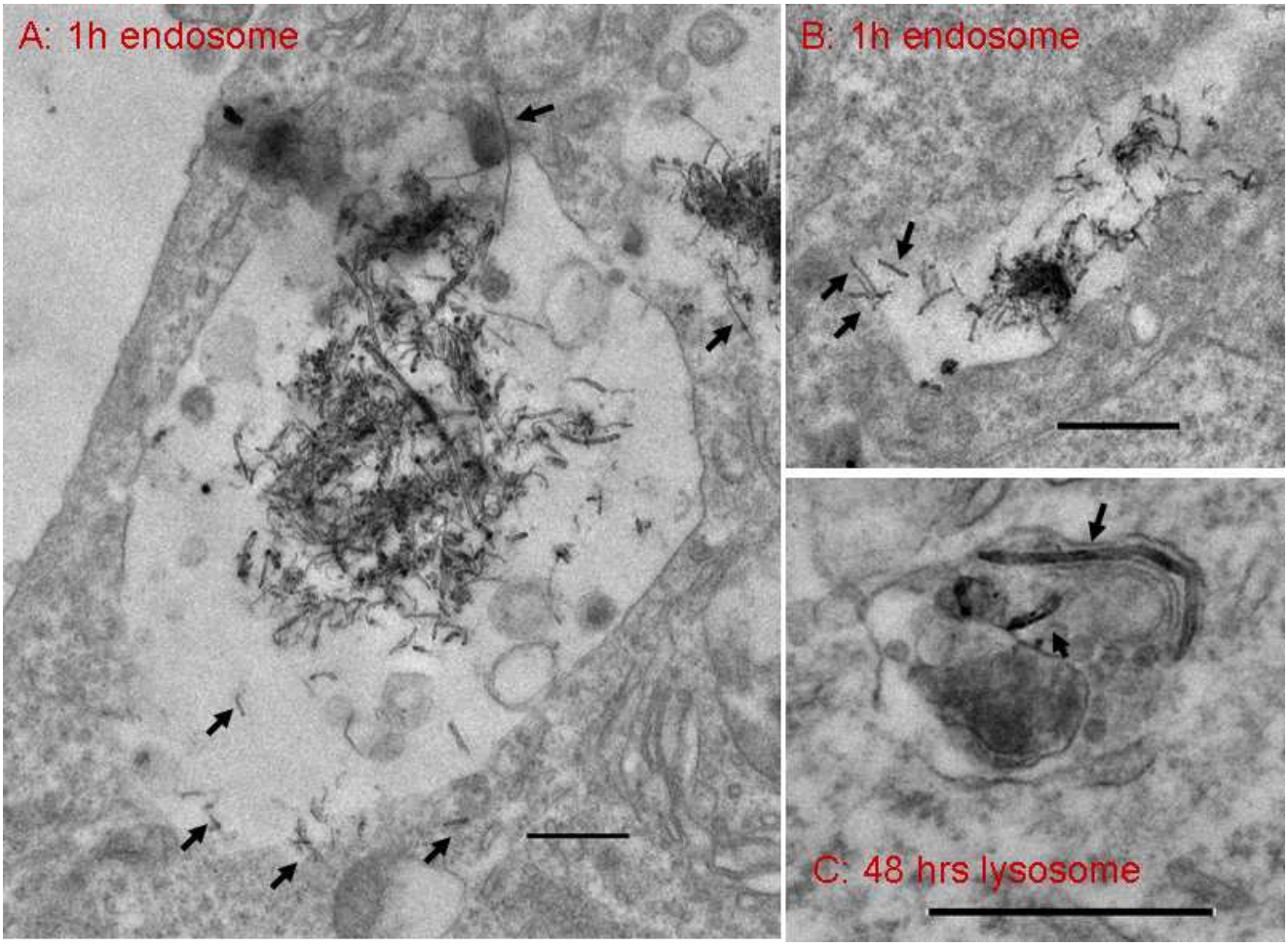

Figure S3. TEM characterization of MWCNT-COOH uptake and cellular locations in HEK293 cells. Cells were incubated with nanotubes (100 μg/mL) for 1 hour and 48 hours at 37°C, respectively. The cells were then fixed, embedded and sectioned followed by imaging. Arrows indicate MWCNT-COOHs. All scale bars represent 500 nm.

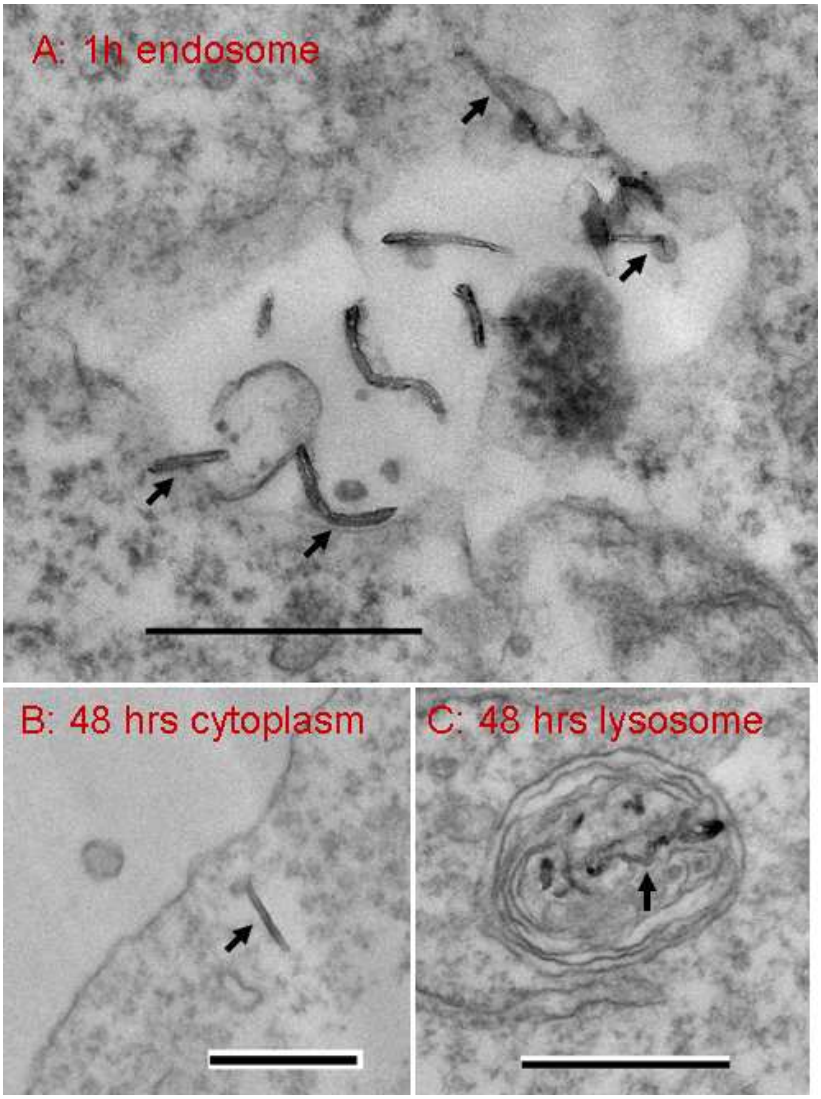

Figure S4. TEM characterization of MWCNT-NH_2 uptake and cellular locations in HEK293 cells. Cells were incubated with nanotubes (100 μg/mL) for 1 hour and 48 hours at 37°C, respectively. The cells were then fixed, embedded and sectioned followed by imaging. Arrows indicate MWCNT-NH_2s. All scale bars represent 500 nm.

Table S1. Identified human plasma proteins bound to MWCNT-COOH and MWCNT-NH_2.

Lipoproteins	**MWCNT-COOH**	**MWCNT-NH2**
Apolipoprotein A-I	**X**	**X**
Apolipoprotein A-II	**X**	**X**
Apolipoprotein A-IV	**X**	**X**
Apolipoprotein B-100	**X**	**X**
Apolipoprotein C-I	**X**	
Apolipoprotein C-II	**X**	**X**
Apolipoprotein C-III	**X**	**X**
Apolipoprotein E	**X**	**X**
Apolipoprotein L1	**X**	**X**
Beta-2-glycoprotein 1 (Apo H)	**X**	
Clusterin (Apo J)	**X**	**X**
Complement System	**MWCNT-COOH**	**MWCNT-NH2**
Complement C1q subcomponent subunit B	**X**	**X**
Complement C1q subcomponent subunit C	**X**	**X**
Complement C3	**X**	**X**
Complement C4-A	**X**	**X**
Complement C5	**X**	
Complement component C8 beta chain	**X**	
Complement component C9	**X**	
Complement factor B	**X**	
Complement factor H	**X**	**X**
Complement factor H-related protein 1	**X**	
Complement factor I	**X**	
Immunoglobin	**MWCNT-COOH**	**MWCNT-NH2**
Ig gamma-1 chain C region	**X**	**X**
Ig gamma-2 chain C region	**X**	
Ig gamma-3 chain C region	**X**	
Ig kappa chain C region	**X**	**X**
Ig kappa chain V-III region SIE	**X**	
Ig lambda chain C regions	**X**	
Ig mu chain C region	**X**	**X**
Coagulation factors	**MWCNT-COOH**	**MWCNT-NH2**
Fibrinogen alpha chain	**X**	**X**
Fibrinogen beta chain	**X**	**X**
Fibrinogen gamma chain	**X**	**X**
Fibronectin	**X**	**X**
Antithrombin-III	**X**	
Coagulation factor IX		**X**
Coagulation factor XI		**X**
Kininogen-1	**X**	**X**
Vitamin K-dependent protein S		**X**
Acute-phase protein	**MWCNT-COOH**	**MWCNT-NH2**
Alpha-1-antitrypsin	**X**	
Cystatin-C	**X**	
Inter-alpha-trypsin inhibitor heavy chain H4	**X**	**X**
Plasma serine protease inhibitor	**X**	
Transthyretin	**X**	**X**

Table S1. *Continue.*

Carrier Proteins	**MWCNT-COOH**	**MWCNT-NH2**
Ceruloplasmin		**X**
Haptoglobin-related protein		**X**
Hemopexin	**X**	
Serotransferrin	**X**	
Serum albumin	**X**	**X**
Others	**MWCNT-COOH**	**MWCNT-NH2**
Alpha-2-HS-glycoprotein	**X**	
Histidine-rich glycoprotein	**X**	**X**
Proteoglycan-4	**X**	
Gelsolin	**X**	
Insulin-like growth factor-binding protein complex acid labile chain	**X**	
Lipopolysaccharide-binding protein	**X**	
Pigment epithelium-derived factor	**X**	
Prothrombin		**X**
Secreted phosphoprotein 24		**X**
Selenoprotein P	**X**	
Serum paraoxonase/arylesterase 1	**X**	**X**
Tetranectin	**X**	
Thrombospondin-4	**X**	
Vitamin D-binding protein		**X**
Vitronectin	**X**	**X**
Zinc finger Ran-binding domain-containing protein 3		**X**